Clinical & Experimental Immunology
The Journal of Translational Immunology

Clinical and Experimental Immunology ORIGINAL ARTICLE doi:10.1111/cei.12134

Genetic deletion of granzyme B does not confer resistance to the development of spontaneous diabetes in non-obese diabetic mice

M. Kobayashi,* C. Kaneko-Koike,† N. Abiru,* T. Uchida,† S. Akazawa,* K. Nakamura,* G. Kuriya,* T. Satoh,* H. Ida,** E. Kawasaki,‡ H. Yamasaki,¶ Y. Nagayama,§ H. Sasaki† and A. Kawakami*

*Department of Endocrinology and Metabolism, Unit of Translational Medicine, Graduate School of Biomedical Science, Departments of †Hospital Pharmacy, ‡Metabolism/Diabetes and Clinical Nutrition and §Molecular Medicine, ¶Center for Health and Communicating Medicine, Nagasaki University, Nagasaki, and **Division of Respirology, Neurology and Rheumatology, Department of Medicine, Kurume University, Kurume, Fukuoka, Japan

Accepted for publication 6 May 2013
Correspondence: N. Abiru, Department of Endocrinology and Metabolism, Unit of Translational Medicine, Graduate School of Biomedical Science, Nagasaki University, 1-7-1 Sakamoto, Nagasaki 852-8501, Japan.
E-mail: abirun@nagasaki-u.ac.jp

Masakazu Kobayashi and Chieko Kaneko-Koike contributed equally to this study.

Summary

Granzyme B (GzmB) and perforin are proteins, secreted mainly by natural killer cells and cytotoxic T lymphocytes that are largely responsible for the induction of apoptosis in target cells. Because type 1 diabetes results from the selective destruction of β cells and perforin deficiency effectively reduces diabetes in non-obese diabetic (NOD) mice, it can be deduced that β cell apoptosis involves the GzmB/perforin pathway. However, the relevance of GzmB remains totally unknown in non-obese diabetic (NOD) mice. In this study we have focused on GzmB and examined the consequence of GzmB deficiency in NOD mice. We found that *NOD.GzmB*$^{-/-}$ mice developed diabetes spontaneously with kinetics similar to those of wild-type NOD (*wt-NOD*) mice. Adoptive transfer study with regulatory T cell (T_{reg})-depleted splenocytes (SPCs) into NOD-SCID mice or *in-vivo* T_{reg} depletion by anti-CD25 antibody at 4 weeks of age comparably induced the rapid progression of diabetes in the *NOD.GzmB*$^{-/-}$ mice and *wt-NOD* mice. Expression of GzmA and Fas was enhanced in the islets from pre-diabetic *NOD.GzmB*$^{-/-}$ mice. In contrast to spontaneous diabetes, GzmB deficiency suppressed the development of cyclophosphamide-promoted diabetes in male NOD mice. Cyclophosphamide treatment led to a significantly lower percentage of apoptotic $CD4^+$, $CD8^+$ and $CD4^+CD25^+$ T cells in SPCs from *NOD.GzmB*$^{-/-}$ mice than those from *wt-NOD* mice. In conclusion, GzmB, in contrast to perforin, is not essentially involved in the effector mechanisms for β cell destruction in NOD mice.

Keywords: apoptosis, NOD mice, transgenic/knock-out mice, type 1 diabetes

Introduction

Type 1 diabetes is characterized by progressive autoimmune destruction of islet β cells with a long prodromal phase [1]. The hallmark of immune-mediated diabetes is T cell-mediated destruction of the insulin-producing β cells in the islets in both humans and the non-obese diabetic (NOD) mouse model of type 1 diabetes [2]. The precise mechanisms of β cell destruction leading to diabetes remain unclear. Many molecules, including Fas ligand (FasL) and cytokines, such as interleukin (IL)-1β, tumour necrosis factor (TNF)-α and interferon (IFN)-γ, cause release of other cytokine mediators that have the potential to damage the β cells [3]. Granzyme B (GzmB) and perforin have been shown to induce cytotoxic T lymphocyte (CTL)-mediated target cell apoptosis [4,5]. Perforin is involved in pore formation across the membranes via a Ca^{2+}-dependent mechanism. This pore enables the entry of serine protease granzymes into the cell, causing the cleavage and activation of several targets, such as effector caspases and the BH3-only protein Bid [6]. Some researchers believe that perforin/granzyme cause the initial β cell insult in diabetes, because spontaneous diabetes and cyclophosphamide (CYP)-induced diabetes are suppressed in perforin knock-out NOD mice [7]. However, the relevance of GzmB remains totally unknown in the pathogenesis of type 1 diabetes.

This study was therefore conducted to investigate the role of GzmB in the pathogenesis of a spontaneous type 1 diabetes model studying the NOD mouse whose disease pathogenesis, specifically in relation to autoimmune-mediated β cell destruction, is most probably similar to that in human type 1 diabetes.

Table 1. Polymorphic markers at known non-obese diabetic (NOD) diabetes susceptibility (idd) loci and genotyping marker of granzyme B (GzmB).

Idd loci/chromozome	Satellite marker	Primer sequence
Idd1/chr17	D17*Mit34*	5′-TGTTGGAGCTGAATACACGC-3′
		5′-GGTCCTTGTTTATTCCCAGTACC-3′
Idd2/chr9	D9*Mit205*	5′AATAGCCTACTCTGGATTCACAGG-3′
		5′-TACCTTCTCCTCTTTGGTTTTTG 3′
Idd3/chr3	D3*Mit95*	5′-CTAAAAGCACTAGCAAAGAAAATCA-3′
		5′-CCTCCACACACATGTCCTTG-3′
Idd4/chr11	D17*Mit34*	5′-ATGAGACCATGCTCCTCCAC-3′
		5′-TTGTCCTCTGACCTTCACACC-3′
Idd5/chr1	D1*Mit18*	5′-TCTGGTTCCAGGCTTGATTC-3′
		5′-TCACAAGTGAGGCTCCAGG-3′
Idd6/chr6	D6*Mit339*	5′-ATATCGATTGGCTTCTAAATGTCA-3′
		5′-GCAGGTTGTCCTCTCACCTC-3′
Idd7/chr7	D7*Mit20*	5′-GTGTAGCAATGGTGTCGGTG-3′
		5′-AAGCCTGCCTCCAGATGTAA-3′
Idd8&12/chr14	D14*Mit222*	5′-GGTCAGTGAGAAGCCCTGTC-3′
		5′-GTCTAACTGCTTTTTTGTGGGG-3′
Idd9&11/chr4	D4*Mit59*	5′-AGAGTTTGGTCTCTTCCCCTG-3′
		5′-TATCCAACACATTTATGTCTGCG-3′
Idd10/chr3	D3*Mit103*	5′-CCAGGGGTGGTGGTCTTAC-3′
		5′-TGTCAGGTGCCCAGGTCT-3′
Idd13/chr2	D2*Mit17*	5′-AGGCAATTACAAGGCCTGG-3′
		5′-CACCCATCTCCCTCAGTCAT-3′
Idd14/chr13	D13*Mit61*	5′-TGCTCCAATACAACAAGGTCC-3′
		5′-CCAGCCAAGGTGTGTTGAC-3′
GzmB/chr14		5′GGACAAAGGCAGGTGAGTAAGCAA-3′
		5′-TTGATGACTGAGTTTGGGGTGAGG-3′
Mutated GzmB	*Neo 0013/0014*	5′-CTTGGGTGGAGAGGCTATTC-3′
		5′-AGGTGAGATGACAGGAGATC-3′

Materials and methods

Mice

Female NOD mice and NOD-severe combined immunodeficient (SCID) mice were purchased from Clea Japan (Tokyo, Japan), and C57BL/6-GzmB-deficient mice (B6·129S2-Gzmb^{tm1Ley}, stock number 002248) were purchased from the Jackson Laboratory (Bar Harbor, ME, USA); all animals were maintained in the Laboratory Animal Center for Biomedical Research at Nagasaki University under specific pathogen-free conditions. All animal experiments described in this study were approved by the institutional animal experimentation committee and were conducted in accordance with the Guidelines for Animal Experimentation.

Establishment of granzyme B-deficient NOD mice

We have established NOD mice with the GzmB gene deleted by back-crossing C57BL/6-GzmB-deficient mice (B6·129S2-Gzmb^{tm1Ley}) with NOD mice. The targeted allele was introgressed into the NOD background using a marker-assisted 'speed congenic' breeding approach, wherein backcross segregants were fixed for homozygosity for NOD alleles at NOD/B6/129 polymorphic markers at known NOD diabetes susceptibility (idd) loci (Table 1). We determined the GzmB knock-out gene utilizing polymerase chain reaction (PCR) amplification to detect the primer's neomycin sequence (Table 1) in the disrupted knock-out gene. We screened an additional four markers on chromosome 14 flanking the GzmB mutation to define the size of the congenic interval. N4 mice were NOD-derived at all markers (iddm 1–14) tested across the genome, except for a congenic interval of less than 5 cM flanking the GzmB-targeted mutation on chromosome 14, thereby excluding the possibility that the presence of the 129S2 genome could contribute resistance at the *Idd8&12* locus on that chromosome. Homozygous GzmB-deficient NOD background mice (*NOD.GzmB*$^{-/-}$) were produced by intercrossing of heterozygotes at N11, and a permanent line of *NOD.GzmB*$^{-/-}$ and wild-type (*wt-NOD*) mice were established at N11.

Monitoring for spontaneous diabetes and cyclophosphamide-promoted diabetes

Blood glucose levels were monitored using One-touch Ultra (Johnson & Johnson, Tokyo, Japan) every other week starting at 12 weeks of age for spontaneous diabetes. For CYP-

promoted diabetes, 200 mg/kg of CYP (Sigma-Aldrich KK, Tokyo, Japan) was injected intraperitoneally (i.p.) at 9 and 11 weeks of age, as described previously [7,8]. Blood glucose levels were monitored at 10 weeks of age and three times a week, starting at 11 weeks of age.

Mice with blood glucose levels above 250 mg/dl for two consecutive measurements were considered diabetic.

Histology

Pancreatic sections were analysed histologically by fixing tissues in 10% formalin and staining the paraffin-embedded samples with haematoxylin and eosin. A minimum of 30 islets from each mouse were observed microscopically by two different observers for the presence of insulitis, and the levels of insulitis were scored according to the following criteria: 0, no lymphocyte infiltration; 1, islets with lymphocyte infiltration in less than 25% of the area; 2, 25–50% of the islet infiltrated; 3, 50–75% of the islet infiltrated; and 4, more than 75% infiltrated or small retracted islets.

Adoptive transfer experiments

Non-diabetic 12–14-week-old donor mice (*NOD.GzmB*$^{-/-}$ or wt-NOD) were killed and their spleens were harvested under sterile conditions. CD25$^+$ T cells were depleted from 12–14-week-old donor mice splenocytes using a CD25 MicroBead Kit (Miltenyi Biotec, Auburn, CA, USA) by Auto-MACS, according to the manufacturer's protocol. CD25$^+$ T cell-depleted splenocytes ($1{\cdot}5 \times 10^7$ per mouse) were injected i.p. into 8–12-week-old NOD-SCID recipient mice. The mice were monitored for blood glucose biweekly after adoptive transfer.

In-vivo regulatory T cell (T_{reg})-depletion by anti-CD25 antibody (PC61)

Anti-CD25 monoclonal antibody was purified from ascites of mice injected i.p. with hybridoma PC61 using a HiTrapTM protein G HP column (Amersham, Piscataway, NJ, USA), as described previously [9]. Five hundred μg of anti-CD25 antibody was injected i.p. at 4 weeks and the blood glucose levels were monitored every week, starting at 10 weeks of age.

Real-time quantitative polymerase chain reaction (PCR)

Islets were isolated from 20-week-old female mice by pancreatic digestion with collagenase (Wako Pure Chemical Industries Ltd, Tokyo, Japan). Islets were purified by Histopaque (Sigma-Aldrich, Tokyo, Japan) density gradient centrifugation. Isolated islets were stored at –80°C until use. Total RNA was extracted from mice islets. cDNA synthesis was performed using primers using the SuperScript III First-strand Synthesis System for reverse transcription (RT)–PCR (Invitrogen, Carlsbad, CA, USA). cDNAs were used as templates in SYBR green real-time PCR assays on a LightCycler (Roche Diagnostics, Tokyo, Japan). The primers used in the PCR reaction for GzmB, granzyme A (GzmA), granzyme C (GzmC), Fas and perforin were obtained from SA Biosciences. Sample data were analysed according to the comparative cycle threshold method and were normalized by stable reference genes of β-actin and glyceraldehyde 3-phosphate dehydrogenase (GAPDH) selected by geNorm visual basic application (VBA) applet among three housekeeping genes, including β-actin, GAPDH and 18S. All results were expressed as a percentage of the value in control extracts.

Apoptosis

Staining for apoptosis was conducted on single-cell suspensions of splenocytes (SPCs). A total of 1×10^6 SPCs were incubated for 15 min at room temperature with 5 μl of annexin V-fluorescein isothiocyanate (FITC), 1 μl of anti-CD4-allophycocyanin (APC) monoclonal antibody (mAb), 1 μl of anti-CD8-APC mAb, 1 μl of anti-CD25-phycoerythin (PE) mAb and 5 μl of propidium iodide (PI). All fluorescein-labelled antibodies were purchased from BD Pharmingen. The result was calculated based on the differences in annexin V percentage between CYP-treated cells and non-CYP-treated cells. All cells were analysed on a FACSCanto II flow cytometry system using FACS Diva software (BD Biosciences, Tokyo, Japan).

Statistics analysis

Group differences were analysed by the Mann–Whitney *U*-test and Student's *t*-test. Differences between Kaplan–Meier survival curves were estimated by the log-rank test, with the use of DR SPSS version 2 for Windows software (SPSS, Inc., Chicago, IL, USA). *P*-values less than 0·05 were considered statistically significant. Insulitis levels were analysed by Ridit analysis, and levels of *t* higher than 1·96 or lower than –1·96 were considered statistically significant.

Results

GzmB deletion did not affect the spontaneous development of diabetes and insulitis

NOD mice develop diabetes after 12 weeks of age, with a higher incidence in females than males [10]. In our colony, 75–85% of female and 10–20% of male NOD mice develop diabetes by age 48 weeks. Using speed congenic techniques with diabetogenic loci (iddm 1–14), we have established

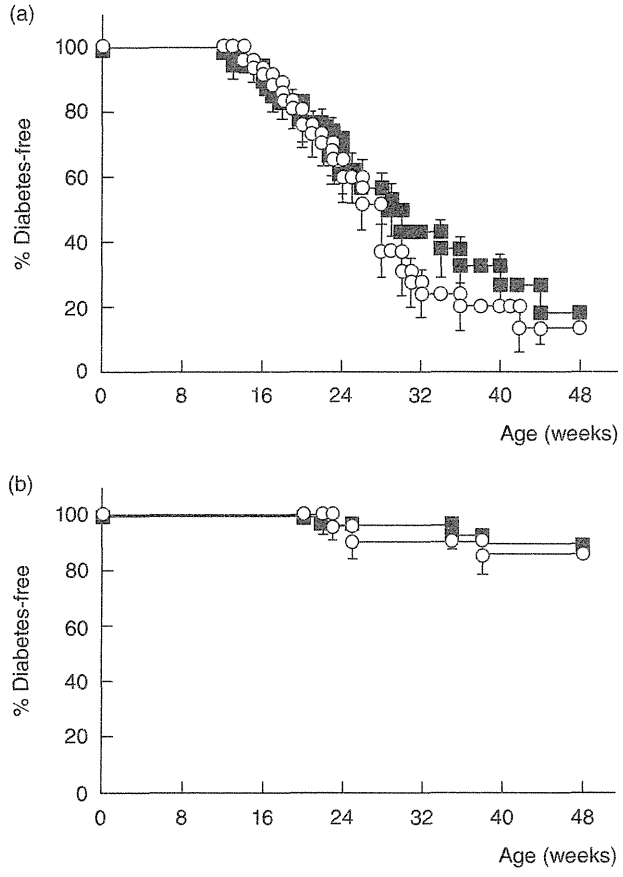

Fig. 1. Life-table analysis for the development of spontaneous diabetes. Blood glucose levels were monitored every week starting at 12 weeks and every other week from 20 weeks. (a) Female mice. Squares: wild-type non-obese diabetic (*wt-NOD*) ($n = 47$). Open circles: *NOD*.granzyme B $(GzmB)^{-/-}$ ($n = 44$). (b) Male mice. Squares: wt-NOD ($n = 27$), open circles: $NOD.GzmB^{-/-}$ ($n = 21$).

NOD mice with GzmB deleted. In the established *wt-NOD* mice, 82% (39 of 47) of female mice and 11% (three of 27) of male mice developed diabetes by age 48 weeks. This implied that 10–11 back-crossed mice become NOD-background from a C57BL/6-background. Among female mice, $NOD.GzmB^{-/-}$ mice became diabetic starting at 14 weeks of age, and *wt-NOD* mice became diabetic starting at 12 weeks of age. The incidence of spontaneous diabetes was essentially identical between these two groups ($P = 0{\cdot}46$) (Fig. 1a). In male mice, $NOD.GzmB^{-/-}$ mice became diabetic starting at 23 weeks of age, and *wt-NOD* mice became diabetic starting at 22 weeks of age. As in female mice, the incidence of spontaneous diabetes was essentially identical between these groups ($P = 0{\cdot}91$) (Fig. 1b). We next compared the levels of the insulitis between female $NOD.GzmB^{-/-}$ and *wt-NOD* mice at 12 weeks of age and found that there were no significant differences between both groups (Ridit score, T = 1·27) (Fig. 2). These results are consistent with the report by Thomas *et al.* [11].

GzmB deficiency did not affect the adoptively transferred diabetes with T_{reg}-depleted SPCs or *in-vivo* T_{reg}-depletion in the NOD mice

Recent reports indicate that GzmB might be a key molecule for the suppressive function in $CD4^+CD25^+$ T_{regs} as well as the function of effector T cells (T_{effs}) for target cell destruction [12]. To investigate the relevance of GzmB in the function of T_{effs} and T_{regs}, we performed an adoptive transfer study involving the transfer of T_{reg}-depleted SPCs and *in-vivo* T_{reg}-depletion in $NOD.GzmB^{-/-}$ mice or *wt-NOD* mice. The NOD-SCID mice transferred with T_{reg}-depleted SPCs from both groups became diabetic starting at 3 weeks of transfer. The incidence of diabetes was 87·5% in the $NOD.GzmB^{-/-}$ mice and 75% in the *wt-NOD* mice at 10 weeks after transfer ($P > 0{\cdot}05$) (Fig. 3a). We also found that T_{reg} depletion by anti-CD25 antibody at 4 weeks of age accelerated diabetes in the $NOD.GzmB^{-/-}$ mice as well as in *wt-NOD* mice and that the course of disease development did not show any significant difference between these groups (Fig. 3b). Taken together, GzmB does not affect the disease pathogenesis in relation not only to β cell destruction by T_{effs}, but also the suppressive function of T_{regs} in NOD mice.

Expression of GzmA and Fas was enhanced in the islets from pre-diabetic $NOD.GzmB^{-/-}$ mice

We evaluated the expression of GzmB in the islets of pre-diabetic $NOD.GzmB^{-/-}$ mice or *wt-NOD* mice. As expected, GzmB was expressed in the islets from pre-diabetic *wt-NOD* mice but not in those from $NOD.GzmB^{-/-}$ mice or NOD-*SCID* mice (Fig. 4). However, there was no significant alteration in the expression levels of GzmB in islets from 12-week-old *wt-NOD* mice and 20-week-old pre-diabetic

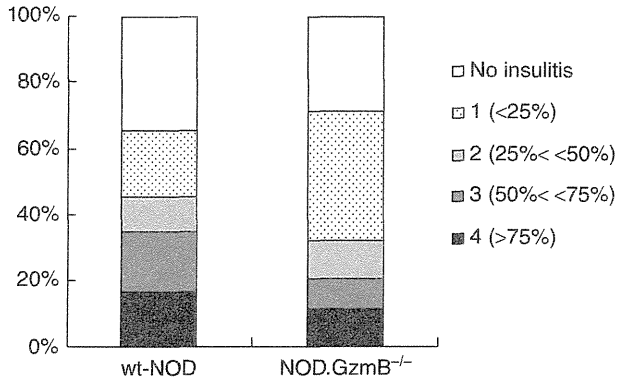

Fig. 2. Histological analysis for insulitis. Levels of insulitis in wild-type non-obese diabetic (*wt-NOD*) mice ($n = 5$) and *NOD*.granzyme B $(GzmB)^{-/-}$ mice ($n = 5$) at 12 weeks of age. A level of T > 1·96 determined by Ridit analysis was regarded as significant. No significant difference was found between the two groups at 12 weeks of age (T = 1·27).

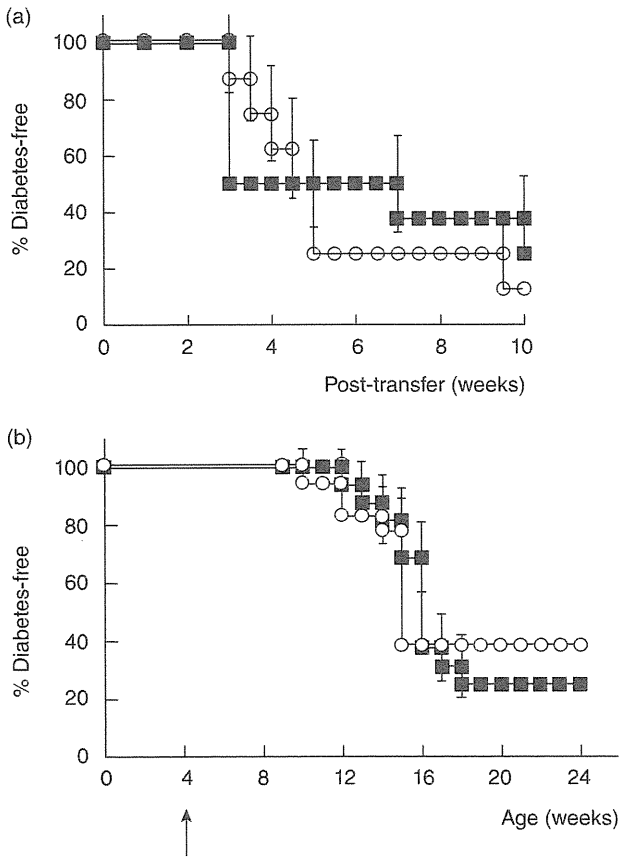

Fig. 3. Adoptive transfer study and the development of diabetes following injection of PC61. (a) $CD25^+$-depleted splenocytes (2×10^7) from non-obese diabetic.granzyme B $(NOD.GzmB)^{-/-}$ ($n = 8$ open circle) and wild-type (*wt*)-*NOD* ($n = 8$ square) mice were transferred into *NOD*-SCID mice. (b) Diabetes-free ratios in *in-vivo* regulatory T cell (T_{reg})-depleted *NOD*.$GzmB^{-/-}$ ($n = 18$ open circle) and *wt-NOD* ($n = 16$ square) following injection of PC61 at 4 weeks of age.

mice. We also investigated the mRNA expression of other apoptosis-associated molecules, including GzmA, GzmC, perforin and Fas in the pre-diabetic *wt-NOD* mice and *NOD.GzmB*$^{-/-}$ mice, to evaluate the mechanism of diabetic induction in *NOD.GzmB*$^{-/-}$mice. Expressions of GzmA and Fas, but not GzmC, were significantly higher in *NOD.GzmB*$^{-/-}$ mice than those in *wt-NOD* mice (GzmA: $P < 0{\cdot}01$, Fas: $P < 0{\cdot}01$). No significant difference in the expression levels of perforin was observed between these groups.

GzmB deficiency suppressed the development of CYP-promoted diabetes in male NOD mice

Injection of CYP induces a rapid rise and high percentage of diabetes in NOD mice of both sexes [8]. CYP was injected twice into *wt-NOD* mice or *NOD.GzmB*$^{-/-}$ mice at 9 and 11 weeks of age. Some of the *wt-NOD* mice developed diabetes on days 9–14 before the second injection, but most became diabetic only after the second injection of CYP between days 21 and 25, with incidences of 60% for female mice and 80% for male mice at 60 days after the first injection. However, in *NOD.GzmB*$^{-/-}$ mice diabetes occurred mainly between days 14 and 25, and the incidence was reduced to 40% for female mice ($P = 0{\cdot}32$) or 30% for male mice compared to those of *wt-NOD* mice ($P = 0{\cdot}0031$) (Fig. 5a,b).

T cells from CYP-treated $GzmB^{-/-}$ mice display reduced apoptosis

Previous study has shown that *in-vivo* blockade of the Fas–Fas ligand pathway also inhibits CYP-promoted diabetes. Interestingly, this protective effect was not due to suppression of β cell apoptosis, but rather to the apoptosis resistance in both $CD4^+$ and $CD8^+$ T cells by the CYP [13]. To verify whether or not NOD T cells from CYP-treated mice showed a comparable functional impairment, we isolated $CD4^+$, $CD8^+$ and $CD4^+CD25^+$ T cells 48 h after CYP dosing and compared them with those cells from untreated littermate controls. Analysis of the proportions of apoptotic cells stained by annexin V after CYP treatment showed a significantly greater percentage of apoptotic $CD4^+$, $CD8^+$ or $CD4^+CD25^+$ T cells in *wt-NOD* mice than in *NOD.GzmB*$^{-/-}$ mice ($CD4^+$: $23{\cdot}82 \pm 3{\cdot}82\%$ *versus* $4{\cdot}36 \pm 1{\cdot}99\%$, $P < 0{\cdot}01$; $CD8^+$: $11{\cdot}64 \pm 6{\cdot}23\%$ *versus* $1{\cdot}94 \pm 5{\cdot}32\%$, $P < 0{\cdot}05$; $CD4^+CD25^+$: $7{\cdot}10 \pm 4{\cdot}66\%$ *versus* $0{\cdot}32 \pm 0{\cdot}35\%$, $P < 0{\cdot}05$) (Fig. 6).

Discussion

Perforin/granzymes cause the initial β cell insult in diabetes, as demonstrated by the fact that spontaneous diabetes and

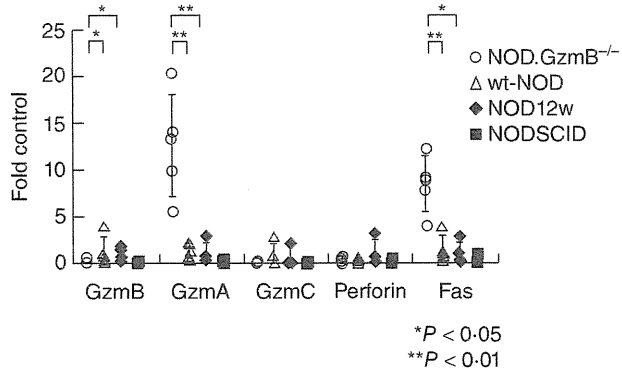

Fig. 4. Real-time reverse transcription–polymerase chain reaction (RT–PCR) analysis of islets in pre-diabetic mice. Real-time RT–PCR of mouse islets at 20 weeks age in wild-type non-obese diabetic (*wt-NOD*) mice, *NOD*.granzyme B $(GzmB)^{-/-}$ mice and NOD-*SCID* mice. Values are the means ± standard error and are expressed as a percentage of the mRNA levels in islets isolated from control 12-week-old *wt-NOD* mice at the same time. *wt-NOD* ($n = 5$), *NOD.GzmB*$^{-/-}$ ($n = 5$).

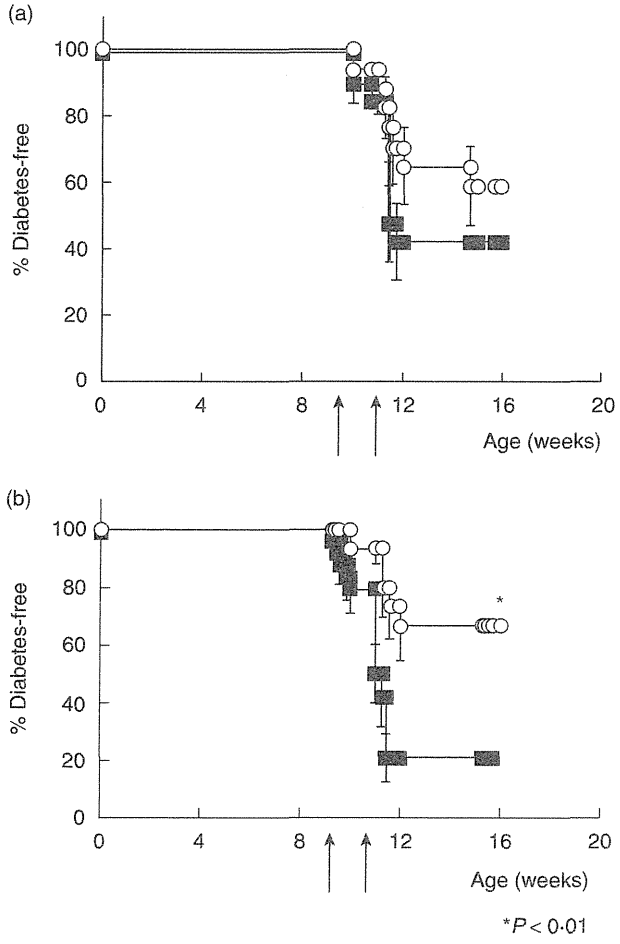

Fig. 5. Life-table analysis for the development of cyclophosphamide (CYP)-promoted diabetes; 200 mg/kg of CYP was injected intraperitoneally (i.p.) at 9 and 11 weeks of age. Blood glucose levels were monitored three times a week starting at 11 weeks of age. (a) Female mice. Squares: wild-type non-obese diabetic (*wt-NOD*) ($n = 19$). Open circles: *NOD*.granzyme B $(GzmB)^{-/-}$ ($n = 17$). (b) Male mice. Squares: *wt-NOD* ($n = 24$). Open circles: $NOD.GzmB^{-/-}$ ($n = 15$).

CYP-induced diabetes were suppressed in perforin knock-out NOD mice [7] while, in a model of viral infection, it has been reported that perforin and granzymes have distinct roles in defensive immunity and immunopathology [14]. We therefore investigated the significance of GzmB on β cell destruction using GzmB-deficient NOD mice. In contrast to perforin-deficient NOD mice, GzmB-deficient NOD mice did not show reduced spontaneous diabetes, consistent with a recent report by Thomas *et al.* [11].

The question then arises as to why GzmB-deficient NOD mice exhibit the distinct phenotype from perforin-deficient NOD mice. In particular, GzmB, but not perforin, is reported to affect not only effector function of CTL but also suppressive function in T_{regs} [12]. One possible explanation for the dissociation between GzmB and perforin is that a reduced suppressive T_{reg} function in GzmB-deficient NOD mice might modify the phenotype of diabetes development.

To evaluate the influence of T_{regs} in our study, we performed an adoptive transfer study with T_{reg}-depleted SPCs to NOD-SCID mice and found that the cells derived from $NOD.GzmB^{-/-}$ mice induced rapid progression of diabetes, a result similar to that of *wt-NOD* mice. We also found that T_{reg} depletion accelerated diabetes in the $NOD.GzmB^{-/-}$ mice as well as *wt-NOD* mice. These results emphasized the conclusion that GzmB is not essentially involved in the effector mechanisms for β cell destruction and might not affect the suppressive function in T_{regs} in the NOD mouse.

Another possible reason for the dissociation is that gene targeting to GzmB, but not to perforin, causes the compensating mechanisms to induce β cell apoptosis when the gene is missing. Of the granzyme family of serine proteases,

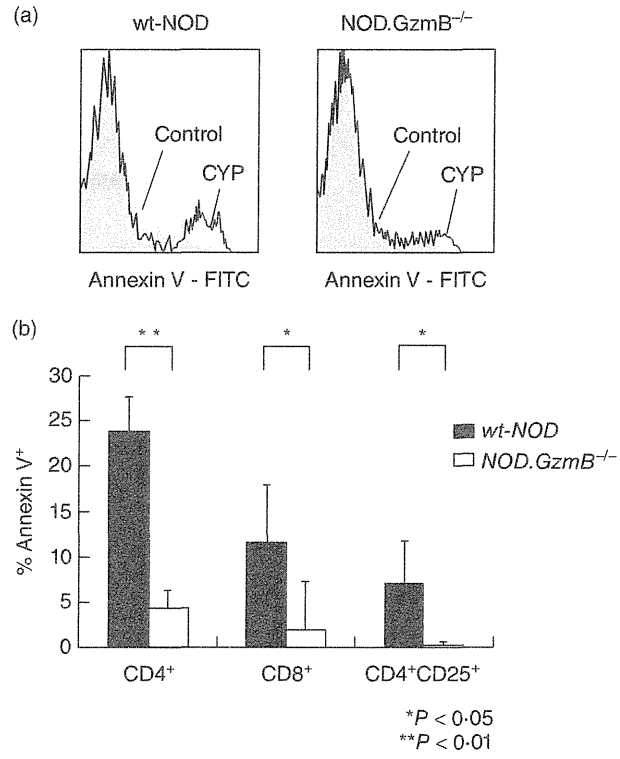

Fig. 6. Effects of cyclophosphamide (CYP) on the apoptosis of $CD4^+$ T cells, $CD8^+$ T cells and $CD4^+CD25^+$ T cells. Wild-type non-obese diabetic (*wt-NOD*) and *NOD*.granzyme B $(GzmB)^{-/-}$ mice were treated with 200 mg/kg CYP intraperitoneally (i.p.) at 8–10 weeks of age, and lymphocytes were prepared from spleens after 48 h for comparison with untreated littermate controls. $CD4^+$ lymphocytes, $CD8^+$ lymphocytes or $CD4^+25^+$ lymphocytes were stained with annexin V^{FITC} as described and analysed by flow cytometry. (a) Staining for apoptosis in $CD4^+$ T cells. Cells were gated initially on forward-scatter (FSC)/side-scatter (SSC) and CD4 expression, excluding all cells staining positive for PI. The percentage of annexin V^+ cells was determined as shown in the histogram overlays. (b) Graphs represent the arithmetic means and values for each individual mouse for the percentage of annexin V^+ $CD4^+$ T cells, annexin V^+ $CD8^+$ T cells and annexin V^+ $CD4^+CD25^+$ T cells in *wt-NOD* ($n = 5$ each), $NOD.GzmB^{-/-}$ ($n = 5$ each).

GzmA and GzmB are the most common in humans and mice. Other granzymes, including H, K and M in humans and C, D, E, F, G, K, L, M and N in mice, are less well characterized [15]. GzmB *in vitro* and GzmA *in-situ* analysis has shown that GzmB and GzmA play important roles in β cell destruction [16,17]. In a previous study using 8·3 T cell receptor (TCR)-transgenic NOD mice, perforin gene knock-out did not alter the development of diabetes [18]. The results of another study indicated that T cells from 8·3 TCR-transgenic NOD mice use both perforin and Fas pathways and that Fas compensates for the β cell killing only when perforin is missing [16]. In our *NOD.GzmB*$^{-/-}$ mice, the mRNA expressions of GzmA and Fas were up-regulated significantly compared to *wt-NOD* mice, indicating that there might be pathways to induce β cell death that can compensate fully for each other when GzmB, but not perforin, is removed in *wt-NOD* mice.

In contrast to spontaneous diabetes development, GzmB deficiency suppressed the incidence of CYP-promoted diabetes in NOD mice. In particular, male *NOD.GzmB*$^{-/-}$ mice were significantly less likely and female *NOD.GzmB*$^{-/-}$ mice showed a tendency to be less likely to develop diabetes compared to *wt-NOD* mice. Previous reports indicated that acceleration of diabetes by CYP was associated with a significant T cell depletion, especially with preferential reduction in CD4$^+$CD25$^+$forkhead box protein 3 (Foxp3)$^+$ T populations following injection [19,20]. In our study, both CD4$^+$, CD8$^+$ and CD4$^+$CD25$^+$ T cells from CYP-treated GzmB$^{-/-}$ mice displayed reduced apoptosis, suggesting that the suppression mechanism in *NOD.GzmB*$^{-/-}$ mice might be associated with apoptosis resistance of T cells rather than deficient effector mechanisms. As a result, GzmB deficiency confers resistance to CYP-promoted diabetes.

In conclusion, GzmB is not involved essentially in the effector mechanisms for β cell destruction in NOD mice. Instead, GzmB probably confers apoptosis resistance to T cells. It is possible that several compensation pathways are associated with β cell destruction in the GzmB-deficient NOD mice. If each single gene is not essential by itself, multiple gene knock-out models might be needed to evaluate the exact mechanism of β cell destruction in NOD mice.

Acknowledgements

This study was supported by research grants from the Japan Society for the Promotion of Science (#21591143, #23791036 and #21790874).

Disclosures

The authors have no financial conflicts of interest.

References

1 Eisenbarth GS. Type I diabetes mellitus. A chronic autoimmune disease. N Engl J Med 1986; **314**:1360–8.

2 Bottazzo GF, Dean BM, McNally JM, MacKay EH, Swift PG, Gamble DR. *In situ* characterization of autoimmune phenomena and expression of HLA molecules in the pancreas in diabetic insulitis. N Engl J Med 1985; **313**:353–60.

3 Kawasaki E, Abiru N, Eguchi K. Prevention of type 1 diabetes: from the view point of beta cell damage. Diabetes Res Clin Pract 2004; **66** (Suppl. 1):S27–32.

4 Lord SJ, Rajotte RV, Korbutt GS, Bleackley RC. Granzyme B: a natural born killer. Immunol Rev 2003; **193**:31–8.

5 Trapani JA, Sutton VR. Granzyme B: pro-apoptotic, antiviral and antitumor functions. Curr Opin Immunol 2003; **15**:533–43.

6 Pirot P, Cardozo AK, Eizirik DL. Mediators and mechanisms of pancreatic beta-cell death in type 1 diabetes. Arq Bras Endocrinol Metabol 2008; **52**:156–65.

7 Kagi D, Odermatt B, Seiler P, Zinkernagel RM, Mak TW, Hengartner H. Reduced incidence and delayed onset of diabetes in perforin-deficient nonobese diabetic mice. J Exp Med 1997; **186**:989–97.

8 Harada M, Makino S. Promotion of spontaneous diabetes in non-obese diabetes-prone mice by cyclophosphamide. Diabetologia 1984; **27**:604–6.

9 Fukushima K, Abiru N, Nagayama Y *et al.* Combined insulin B:9-23 self-peptide and polyinosinic–polycytidylic acid accelerate insulitis but inhibit development of diabetes by increasing the proportion of CD4+Foxp3+ regulatory T cells in the islets in non-obese diabetic mice. Biochem Biophys Res Commun 2008; **367**:719–24.

10 Makino S, Kunimoto K, Muraoka Y, Mizushima Y, Katagiri K, Tochino Y. Breeding of a non-obese, diabetic strain of mice. Jikken Dobutsu 1980; **29**:1–13.

11 Mollah ZU, Graham KL, Krishnamurthy B *et al.* Granzyme B is dispensable in the development of diabetes in non-obese diabetic mice. PLoS ONE 2012; **7**:e40357.

12 Gondek DC, Lu LF, Quezada SA, Sakaguchi S, Noelle RJ. Cutting edge: contact-mediated suppression by CD4+CD25+ regulatory cells involves a granzyme B-dependent, perforin-independent mechanism. J Immunol 2005; **174**:1783–6.

13 Mahiou J, Walter U, Lepault F, Godeau F, Bach JF, Chatenoud L. *In vivo* blockade of the Fas–Fas ligand pathway inhibits cyclophosphamide-induced diabetes in NOD mice. J Autoimmun 2001; **16**:431–40.

14 van Dommelen SL, Sumaria N, Schreiber RD, Scalzo AA, Smyth MJ, Degli-Esposti MA. Perforin and granzymes have distinct roles in defensive immunity and immunopathology. Immunity 2006; **25**:835–48.

15 Bolitho P, Voskoboinik I, Trapani JA, Smyth MJ. Apoptosis induced by the lymphocyte effector molecule perforin. Curr Opin Immunol 2007; **19**:339–47.

16 Estella E, McKenzie MD, Catterall T *et al.* Granzyme B-mediated death of pancreatic beta-cells requires the proapoptotic BH3-only molecule bid. Diabetes 2006; **55**:2212–9.

17 Mueller C, Held W, Imboden MA, Carnaud C. Accelerated beta-cell destruction in adoptively transferred autoimmune diabetes correlates with an increased expression of the genes coding for TNF-alpha and granzyme A in the intra-islet infiltrates. Diabetes 1995; **44**:112–7.

18 Amrani A, Verdaguer J, Anderson B, Utsugi T, Bou S, Santamaria P. Perforin-independent beta-cell destruction by diabetogenic

CD8(+) T lymphocytes in transgenic nonobese diabetic mice. J Clin Invest 1999; **103**:1201–9.

19 Gregori S, Giarratana N, Smiroldo S, Adorini L. Dynamics of pathogenic and suppressor T cells in autoimmune diabetes development. J Immunol 2003; **171**:4040–7.

20 Brode S, Raine T, Zaccone P, Cooke A. Cyclophosphamide-induced type-1 diabetes in the NOD mouse is associated with a reduction of CD4+CD25+Foxp3+ regulatory T cells. J Immunol 2006; **177**:6603–12.

World Journal of Gastroenterology

Online Submissions: http://www.wjgnet.com/esps/
wjg@wjgnet.com
doi:10.3748/wjg.v19.i23.3693

World J Gastroenterol 2013 June 21; 19(23): 3693-3698
ISSN 1007-9327 (print) ISSN 2219-2840 (online)

CASE REPORT

Polyarteritis nodosa clinically mimicking nonocclusive mesenteric ischemia

Tsuyoshi Shirai, Hiroshi Fujii, Shinichiro Saito, Tomonori Ishii, Hideyuki Yamaya, Shigehito Miyagi, Satoshi Sekiguchi, Naoki Kawagishi, Masato Nose, Hideo Harigae

Tsuyoshi Shirai, Hiroshi Fujii, Shinichiro Saito, Tomonori Ishii, Hideo Harigae, Department of Hematology and Rheumatology, Tohoku University Graduate School of Medicine, Sendai 980-8574, Japan
Hideyuki Yamaya, Shigehito Miyagi, Satoshi Sekiguchi, Naoki Kawagishi, Division of Advanced Surgical Science and Technology, Tohoku University Graduate School of Medicine, Sendai 980-8574, Japan
Masato Nose, Department of Histopathology, Tohoku University Graduate School of Medicine, Sendai 980-8574, Japan
Author contributions: Shirai T reviewed the literature, collected information, provided patient care, and wrote the manuscript; Fujii H, Saito S, Ishii T, Yamaya H, Miyagi S, Sekiguchi S, and Kawagishi N were involved in different stages of the diagnosis, care, and management of the patient, and revised and approved the final draft; Nose M provided the discussion of the pathology, revised and approved the final draft; Harigae H also supervised the entire process from drafting the paper to submission of the final manuscript.
Correspondence to: Tsuyoshi Shirai, MD, PhD, Department of Hematology and Rheumatology, Tohoku University Graduate School of Medicine, 1-1 Seiryo-cho, Aoba-ku, Sendai, Miyagi 980-8574, Japan. tsuyoshirajp@med.tohoku.ac.jp
Telephone: +81-22-7177165 Fax: +81-22-7177497
Received: February 9, 2013 Revised: April 8, 2013
Accepted: April 13, 2013
Published online: June 21, 2013

Abstract

Here, we present the case of a 74-year-old Japanese man with segmental intestinal necrosis, which developed after treatment with pulsed methylprednisolone for mononeuritis multiplex. The patient was weakly positive for myeloperoxidase (MPO)-anti-neutrophil cytoplasmic antibody (ANCA). Computed tomography and surgical findings were compatible with nonocclusive mesenteric ischemia (NOMI). He underwent small intestinal resection by emergency surgery and an intestinal fistula was made. Pathologically, necrotizing vasculitis with fibrinoid necrosis was present in medium to small-sized arteries, which was equivalent to Arkin's classification Ⅱ-Ⅳ. Most of the arteries had fibrous intimal thickening, which was considered to obstruct the arteries and thus cause segmental intestinal necrosis. A diagnosis of polyarteritis nodosa (PAN) was made, and intravenous cyclophosphamide pulse therapy was added to the therapeutic regimen. This patient was successfully treated with these multidisciplinary therapies and his stoma was finally closed. This is a very rare and indicative case of PAN weakly positive for MPO-ANCA and clinically mimicking NOMI, which occurred even after treatment with pulsed methylprednisolone.

Key words: Anti-neutrophil cytoplasmic antibody; Intestinal necrosis; Myeloperoxidase; Nonocclusive mesenteric ischemia; Polyarteritis nodosa

Core tip: We present a patient with polyarteritis nodosa (PAN) weakly positive for myeloperoxidase-anti-neutrophil cytoplasmic antibody and clinically mimicking nonocclusive mesenteric ischemia (NOMI), which occurred after treatment with pulsed methylprednisolone for mononeuritis multiplex. The present case is not only rare but also informative, because vasculitis in medium to small-sized arteries was shown to take a few months to develop tangible signs of visceral ischemia, which can occur even after treatment with pulsed methylprednisolone, and the imaging and surgical findings of intestinal necrosis caused by PAN may resemble those of NOMI.

Shirai T, Fujii H, Saito S, Ishii T, Yamaya H, Miyagi S, Sekiguchi S, Kawagishi N, Nose M, Harigae H. Polyarteritis nodosa clinically mimicking nonocclusive mesenteric ischemia. *World J Gastroenterol* 2013; 19(23): 3693-3698 Available from: URL: http://www.wjgnet.com/1007-9327/full/v19/i23/3693.htm DOI: http://dx.doi.org/10.3748/wjg.v19.i23.3693

INTRODUCTION

Polyarteritis nodosa (PAN) is necrotizing arteritis of medium to small-sized arteries without glomerulonephritis or vasculitis in arterioles, capillaries, or venules[1]. PAN can show a wide variety of symptoms, including general symptoms, neurological manifestations, skin involvement, renal involvement, and gastrointestinal (GI) manifestations[2]. Clinically, the spectrum of GI manifestations is wide, ranging from mild transient abdominal pain to life-threatening complications requiring emergency surgery, *e.g.*, peritonitis, bowel infarction, or hemorrhage[3]. Severe GI involvements, including bowel perforation, bleeding, and pancreatitis, are independent predictive factors for poor prognosis of PAN together with age[4]. Although GI ischemia has been reported to occur at a rate of 13%-31% in PAN patients[3,5], the prevalence of PAN itself is very low, and clinical suspicion of vasculitis is sometimes difficult in cases showing intestinal necrosis. Here, we describe a case in which a patient with PAN presented with segmental intestinal necrosis clinically mimicking nonocclusive mesenteric ischemia (NOMI) even after treatment with pulsed methylprednisolone for vasculitis.

CASE REPORT

A 74-year-old Japanese man was admitted to our hospital because of mononeuritis multiplex in the left ulnar and peroneal nerves on May 26, 2012. Two months previously, he had experienced systemic muscular pain. A tentative diagnosis of polymyalgia rheumatica was made and he was treated with prednisolone (PSL) at 10 mg/d. Although steroids were partially effective in improving the patient's condition, the levels of C-reactive protein (CRP) continued to be high (18 mg/dL). He was referred to our hospital for further evaluation one month later, at which time he had no complaints other than muscular pain. His height was 172 cm and body weight was 62 kg; the patient's body weight had decreased by 3 kg from the onset of the disease. Laboratory tests indicated leukocytosis, anemia, thrombocytosis, and elevated CRP levels. The results of urine tests were negative. The patient was negative for anti-nuclear antibody and proteinase 3 (PR3)-anti-neutrophil cytoplasmic antibody (ANCA), but weakly positive for myeloperoxidase (MPO)-ANCA (23.7 U/mL: normal range 0.0-8.9 U/mL). Tests for infections, including hepatitis B surface antigen and blood culture, were negative. Torso computed tomography (CT) revealed emphysema alone, and whole-body positron emission tomography yielded negative results. Although we recommended hospitalization for diagnosis and treatment, the patient refused for personal reasons. One week later, he noticed numbness in his left hand and leg. He then developed left foot drop, so underwent a medical examination and was admitted to our hospital. On admission, his consciousness was clear, performance status was 3, body temperature was 36.3 ℃, and blood pressure was 178/124 mmHg. He had general muscle weakness and sensory loss in regions supplied by the left ulnar and peroneal nerves, and dorsiflexion of the left foot was compromised to manual muscle testing 2/5. Laboratory tests indicated elevated levels of CRP and muscular enzymes, such as creatine kinase (CK) (Table 1). Urinary analysis showed proteinuria and hematuria with a few casts. He received pulsed methylprednisolone at a dose of 1 g for 3 d followed with PSL at 60 mg/d because the underlying disease was considered to be vasculitis, and intravenous nicardipine for hypertension, which was considered to be caused by renal vascular involvement. Despite this therapy, the CRP level did not fall below 10 mg/dL and the CK level increased significantly to 9358 IU/L after 3 d of this treatment (Figure 1). At the same time, the patient complained of abdominal pain. His abdomen was flat and soft, and showed left lower quadrant pain without muscular defense or rebound. Abdominal X-ray showed a distended intestine, indicating paralytic ileus. CT revealed distended small bowel loops, gas in the small bowel, and blurred enhancement of the intestinal wall without any significant obstruction in the mesenteric arteries, suggesting NOMI (Figure 2A-C). Emergency surgery was performed on the same day. His jejunum to ileum showed segmental ischemia and necrosis over 2 m, and surgical findings were compatible with NOMI (Figure 2D). Small intestinal resection was performed and an intestinal fistula was made. Pathologically, necrotizing vasculitis with fibrinoid necrosis was present in medium to small-sized arteries, and most of the arteries had fibrous intimal thickening (Figure 3). There was no necrotizing vasculitis in arterioles, capillaries, or venules. Pathology was equivalent to Arkin's classification II-IV[6], and a diagnosis of PAN was made. Intravenous cyclophosphamide (IVCY) pulse therapy at a dose of 500 mg/mo was added to the treatment regimen. Although various complications occurred, including deep vein thrombosis, stoma trouble, and disseminated varicella zoster virus infection, the patient recovered well and was transferred to a different hospital for rehabilitation. As his nutritional status had improved because he became able to eat a regular diet without supplemental nutrition, his stoma was closed in April 2013. He is now in complete remission with the dose of PSL tapered to 10 mg/d.

DISCUSSION

NOMI is an acute mesenteric circulatory disorder that is not caused by organic occlusion of blood vessels[7]. The typical patient is critically ill, with severe cardiac disease or sepsis[8]. With regard to pathogenesis, intestinal vasospasm due to persistent low perfusion is thought to cause ischemic disorder due to decreased cardiac output and blood pressure[9]. Mitsuyoshi *et al*[7] reported findings that may be useful as supplemental information in diagnosis of NOMI: (1) enhancement of principal arteries could be traced to the periphery close to the marginal arteries in CT slices; and (2) the staining intensity varied in the intestinal wall in the same slice (showing a difference between regions of the intestinal wall with good and poor

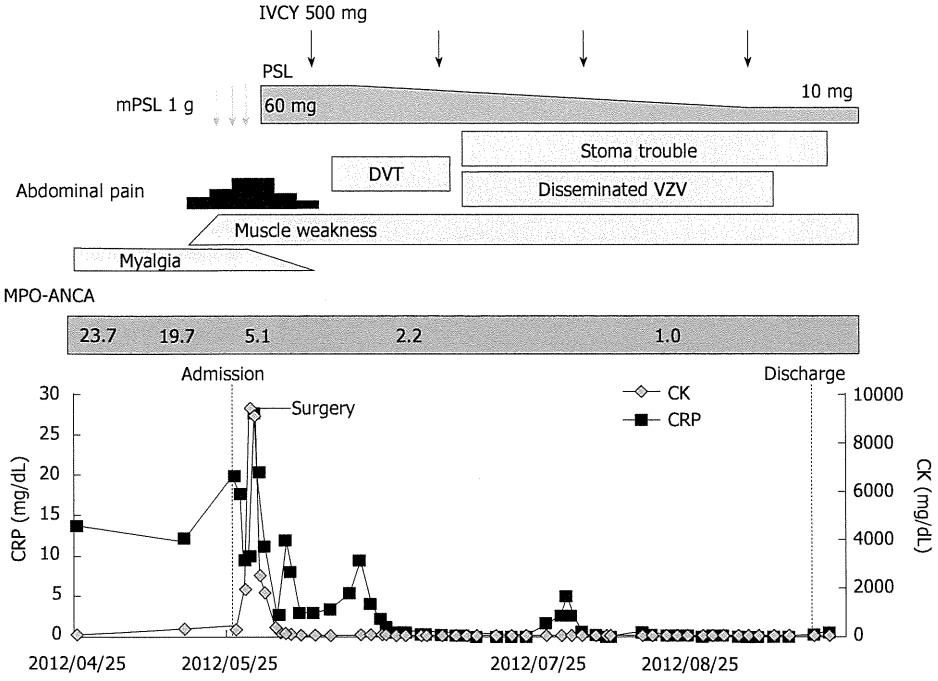

Figure 1 Clinical course. CK: Creatinine kinase; CRP: C-reactive protein; DVT: Deep venous thrombosis; IVCY: Intravenous cyclophosphamide; mPSL: Methylprednisolone; MPO-ANCA: Myeloperoxidase-anti-neutrophil cytoplasmic antibody; PSL: Prednisolone; VZV: Varicella zoster virus.

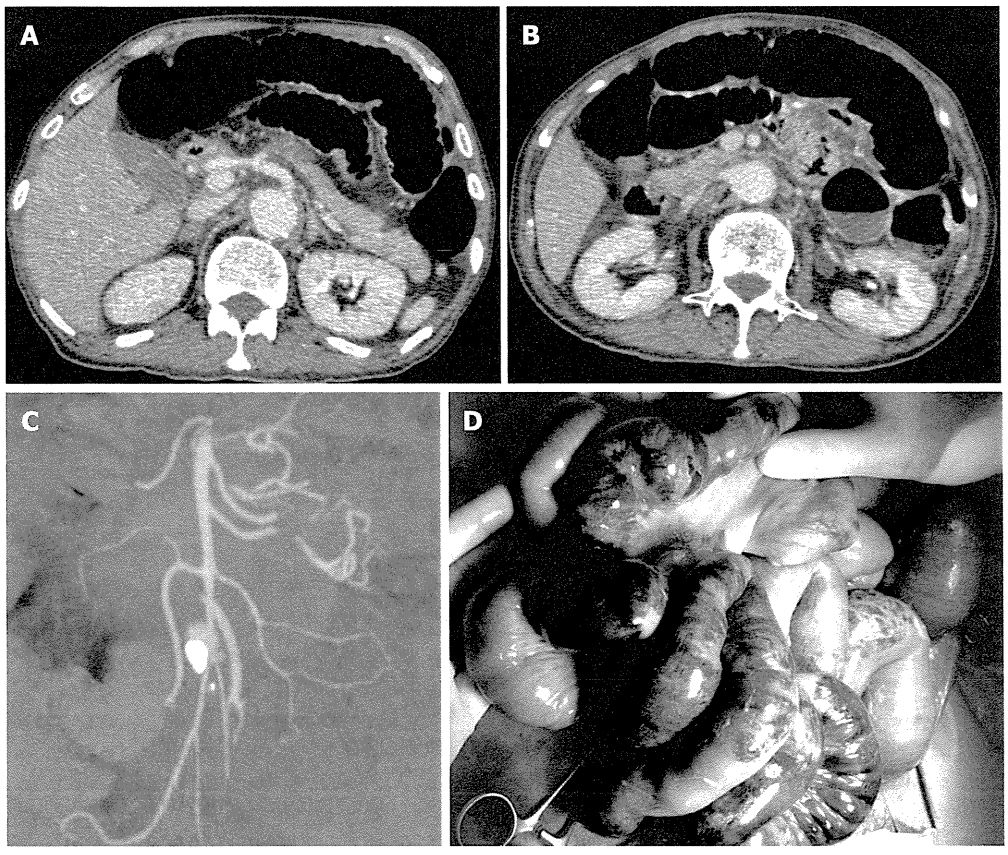

Figure 2 Clinical imaging. A: Computed tomography (CT) image of the abdomen showing distended small bowel loops, gas in the small bowel, blurred enhancement of the intestinal wall, and absence of any significant obstruction in the celiac trunk; B: CT image of the abdomen showing superior mesenteric artery; C: CT angiographic reconstruction of the superior mesenteric artery; D: Surgical findings showing distended small intestine, segmental intestinal ischemia, and necrosis.

blood flow). With regard to laparotomic characteristics, mesenteric blood flow may be retained, even in marginal arteries reaching the lesions, despite extensive necrotization throughout the intestine (noncontinuous segmental necrosis). This was reported to be a marked distinguishing feature from mesenteric thrombosis, in which the mesentery and intestine are necrotized from the site of the thrombus, forming a sphenoidal necrotic area in the region served by the artery (continuous necrosis)[7].

Although CT imaging and surgical findings were compatible with NOMI in this case, the underlying disease was considered to be vasculitis because this patient manifested general weakness, myalgia, and mononeuritis multiplex; clinically apparent mononeuritis multiplex can be a diagnostic or classification criterion for vasculitis affecting peripheral nerves without the need for a nerve

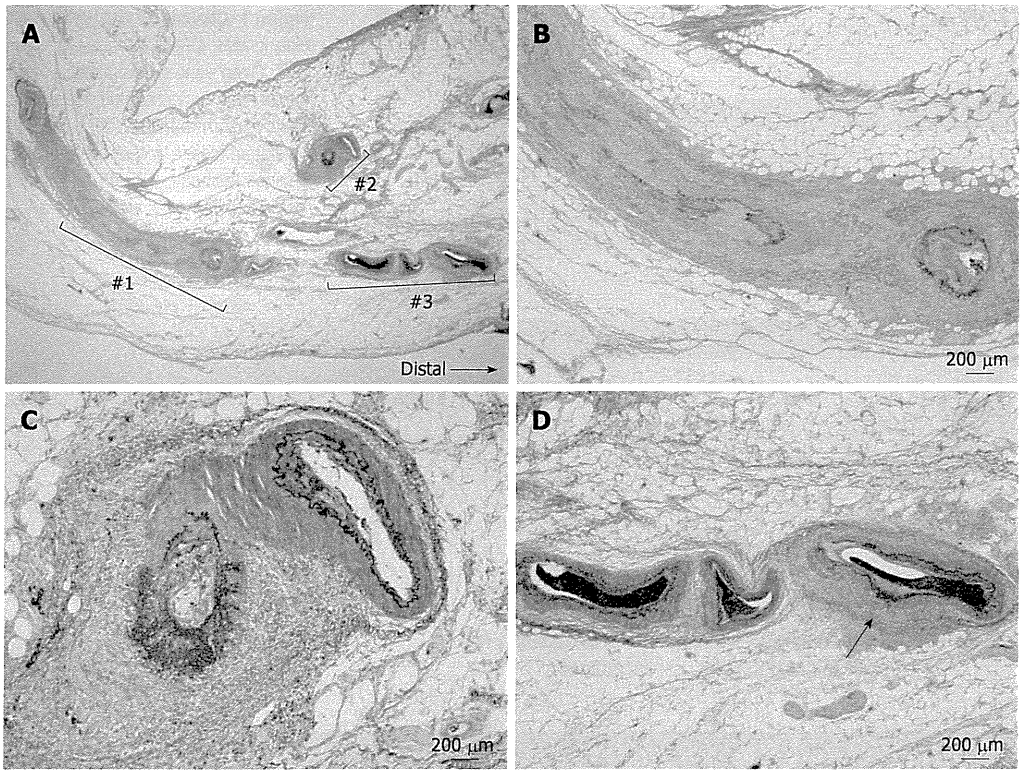

Figure 3 Histological findings of the jejunum. A: Necrotizing vasculitis of the mesenteric artery showing nodular lesions in various stages of the Arkin classification, Elastica-Masson staining; B: Higher magnification of No. 1 in A showing necrotizing vasculitis of mesenteric artery in stage Ⅱ-Ⅲ; C: Higher magnification of No. 2 in A showing necrotizing vasculitis of the mesenteric artery in stage Ⅱ and panarterial necrosis with fibrinoid degeneration; D: Higher magnification of No. 3 in A showing necrotizing vasculitis of mesenteric artery in stage Ⅱ, characterized by destruction of internal elastic lamina associated with fibrinoid necrosis (arrow).

biopsy to observe the vasculitis histologically[10]. In this case, necrotizing vasculitis with fibrinoid necrosis was pathologically present in medium to small-sized arteries, and fibrous intimal thickening was considered to obstruct these arteries and cause segmental intestinal necrosis. Although the pathology was equivalent to Arkin's classification Ⅱ-Ⅳ, most belonged to Arkin's classification Ⅲ-Ⅳ, indicating longstanding vasculitis. Therefore, it is reasonable to consider that the patient suffered from vasculitis from the beginning. Although he was treated with pulsed methylprednisolone before the onset of abdominal symptoms, fibrous intimal thickening of medium to small-sized intestinal arteries must have already occurred.

According to the Chapel Hill Consensus Conference 2012[10], PAN is defined as necrotizing arteritis of medium to small-sized arteries without glomerulonephritis or vasculitis in arterioles, capillaries, or venules, and is not associated with ANCA, which was based on the report that ANCA was typically absent in patients with PAN[11]. In this previous report by Guillevin *et al*[11], one patient (Table 1, No. 40) diagnosed with PAN had MPO-ANCA. Furthermore, there have been some reports presenting pathologically diagnosed PAN with MPO-ANCA positivity, all of which were reported from Japan[12-16]. The prevalence rates of ANCA and ANCA-associated vasculitis are different between Japan and Europe; microscopic polyangiitis (MPA) and MPO-ANCA are more common in Japan, while granulomatosis with polyangiitis and PR3-ANCA are more common in Europe[17,18]. These trends may be related to the reports of PAN with MPO-ANCA positivity in Japan.

Although MPO-ANCA was also weakly positive in this case, this patient clearly fulfilled the American College of Rheumatology 1990 criteria for classification of PAN[19], the pathological findings were typical of PAN as shown in Figure 3, and vasculitis was absent in arterioles, capillaries, and venules. Therefore, a diagnosis of PAN was made in this case. Tanaka *et al*[14] described a case of PAN with MPO-ANCA and vasculitis in mesenteric medium-sized arteries, which was confirmed by autopsy. In their case, the titer of MPO-ANCA was low and was not correlated with the severity of PAN. These points were similar to our case, and we speculated that the epitope and pathogenicity may be different from those of MPO-ANCA found in MPA. Peripheral nervous system vasculitis, hypertension, cutaneous lesions, and myalgias were reported to be more common in PAN with than without GI involvement[5], and our patient also manifested most of these symptoms with the exception of cutaneous lesions.

The standard regimen for PAN, not related to hepatitis B virus infection, is based on a combination of corticosteroids (CS) and CY[20]. The addition of CY to CS particularly benefits patients presenting with factors associated with poor prognosis, such as GI involvement. Intermittent pulse-therapy may be as efficacious as oral CY for inducing remission, while generating fewer side effects. Treating PAN patients positive for factors associated with poor prognosis with 12 rather than 6 CY pulses significantly decreased the relapse rate and significantly increased the probability of event-free survival[20]. Plasma exchange can be prescribed for severe life-threatening PAN as combined rescue therapy, although trials have not proven its benefits when prescribed systematically for all patients with PAN[21].

In addition, the surgical management of patients with acute abdominal syndromes has also improved, and now

Table 1 Laboratory findings

	May 2012	Pre-surgery	Post-surgery	Mar 2013
Urinalysis				
Protein	1+	2+	1+	-
Occult blood	3+	3+	3+	-
Red blood cell	5-9/HPF	5-9/HPF	5-9/HPF	-
Casts	+	+	+	-
Granular	< 4/HPF	< 4/HPF	< 4/HPF	
WBC (/μL)	23700	40700	20800	9500
Segmented cells	89%	87%	93%	56%
Band cells	0%	6%	0%	0%
Eosinophils	3%	0%	0%	1%
Basophils	0%	0%	0%	0%
Lymphocytes	6%	2%	5%	33%
Monocytes	2%	5%	2%	10%
Hb (g/dL)	11.5	11.4	8.4	10.1
PLT (10^4/μL)	49.1	32.8	22.7	24.1
T-Bil (mg/dL)	0.6	1.1	0.8	1.3
AST (IU/L)	39	352	89	36
ALT (IU/L)	32	181	107	45
LDH (IU/L)	304	641	427	217
ALP (IU/L)	368	403	301	326
CK (IU/L)	374	9063	1796	23
TP (g/dL)	6.0	5.6	5.3	5.1
Alb (g/dL)	2.1	2.1	2.6	3.0
BUN (mg/dL)	40	60	52	18
Cr (mg/dL)	0.98	1.11	1.02	1.00
CRP (mg/dL)	19.7	27.6	11.0	0.1
MPO-ANCA (U/mL)	19.2	5.1		Negative

HPF: High-power field; WBC: White blood cells; Hb: Hemoglobin; PLT: Platelets; T-Bil: Total bilirubin; AST: Aspartate aminotransferase; ALT: Alanine aminotransferase; LDH: Lactate dehydrogenase; ALP: Alkaline phosphatase; CK: Creatine kinase; TP: Total protein; Alb: Albumin; BUN: Blood urea nitrogen; Cr: Creatinine; CRP: C-reactive protein; MPO: Myeloperoxidase; ANCA: Anti-neutrophil cytoplasmic antibody.

includes more aggressive surgical management, bowel rest, parenteral nutrition, intensive care unit support, and better wound care[5]. This patient was successfully treated with these multidisciplinary therapies, including emergency surgery followed by PSL and IVCY against PAN. Although small intestinal stoma, central venous catheter, sub nutrition, and immunosuppressive therapy caused many life-threatening complications, close monitoring and appropriate treatment resulted in complete remission of PAN and eventual closure of his stoma.

In conclusion, vasculitis in medium to small-sized arteries takes a few months to show tangible signs of visceral ischemia, and the CT and surgical findings of intestinal necrosis caused by PAN may resemble those of NOMI. Clinical awareness of vasculitis and ANCA measurement (never exclusive) are important in managing patients showing segmental intestinal necrosis.

ACKNOWLEDGMENTS

We thank the staff of the Department of Hematology and Rheumatology, Tohoku University, for help and discussion.

REFERENCES

1 **Jennette JC**, Falk RJ, Andrassy K, Bacon PA, Churg J, Gross WL, Hagen EC, Hoffman GS, Hunder GG, Kallenberg CG. Nomenclature of systemic vasculitides. Proposal of an international consensus conference. *Arthritis Rheum* 1994; **37**: 187-192 [PMID: 8129773]

2 **Pagnoux C**, Seror R, Henegar C, Mahr A, Cohen P, Le Guern V, Bienvenu B, Mouthon L, Guillevin L. Clinical features and outcomes in 348 patients with polyarteritis nodosa: a systematic retrospective study of patients diagnosed between 1963 and 2005 and entered into the French Vasculitis Study Group Database. *Arthritis Rheum* 2010; **62**: 616-626 [PMID: 20112401 DOI: 10.1002/art.27240]

3 **Pagnoux C**, Mahr A, Cohen P, Guillevin L. Presentation and outcome of gastrointestinal involvement in systemic necrotizing vasculitides: analysis of 62 patients with polyarteritis nodosa, microscopic polyangiitis, Wegener granulomatosis, Churg-Strauss syndrome, or rheumatoid arthritis-associated vasculitis. *Medicine* (Baltimore) 2005; **84**: 115-128 [PMID: 15758841]

4 **Guillevin L**, Pagnoux C, Seror R, Mahr A, Mouthon L, Le Toumelin P. The Five-Factor Score revisited: assessment of prognoses of systemic necrotizing vasculitides based on the French Vasculitis Study Group (FVSG) cohort. *Medicine* (Baltimore) 2011; **90**: 19-27 [PMID: 21200183 DOI: 10.1097/MD.0b013e318205a4c6]

5 **Levine SM**, Hellmann DB, Stone JH. Gastrointestinal involvement in polyarteritis nodosa (1986-2000): presentation and outcomes in 24 patients. *Am J Med* 2002; **112**: 386-391 [PMID: 11904113]

6 **Arkin A**. A Clinical and Pathological Study of Periarteritis Nodosa: A Report of Five Cases, One Histologically Healed. *Am J Pathol* 1930; **6**: 401-426. 5 [PMID: 19969916]

7 **Mitsuyoshi A**, Obama K, Shinkura N, Ito T, Zaima M. Survival in nonocclusive mesenteric ischemia: early diagnosis by multidetector row computed tomography and early treatment with continuous intravenous high-dose prostaglandin E(1). *Ann Surg* 2007; **246**: 229-235 [PMID: 17667501]

8 **Björck M**, Wanhainen A. Nonocclusive mesenteric hypoperfusion syndromes: recognition and treatment. *Semin Vasc Surg* 2010; **23**: 54-64 [PMID: 20298950 DOI: 10.1053/j.semvascsurg.2009.12.009]

9 **Bassiouny HS**. Nonocclusive mesenteric ischemia. *Surg Clin North Am* 1997; **77**: 319-326 [PMID: 9146715]

10 **Jennette JC**, Falk RJ, Bacon PA, Basu N, Cid MC, Ferrario F, Flores-Suarez LF, Gross WL, Guillevin L, Hagen EC, Hoffman GS, Jayne DR, Kallenberg CG, Lamprecht P, Langford CA, Luqmani RA, Mahr AD, Matteson EL, Merkel PA, Ozen S, Pusey CD, Rasmussen N, Rees AJ, Scott DG, Specks U, Stone JH, Takahashi K, Watts RA. 2012 revised International Chapel Hill Consensus Conference Nomenclature of Vasculitides. *Arthritis Rheum* 2013; **65**: 1-11 [PMID: 23045170 DOI: 10.1002/art.37715]

11 **Guillevin L**, Lhote F, Amouroux J, Gherardi R, Callard P, Casassus P. Antineutrophil cytoplasmic antibodies, abnormal angiograms and pathological findings in polyarteritis nodosa and Churg-Strauss syndrome: indications for the classification of vasculitides of the polyarteritis Nodosa Group. *Br J Rheumatol* 1996; **35**: 958-964 [PMID: 8883433]

12 **Bohgaki T**, Mukai M, Notoya A, Kohno M. [Two cases of classical polyarteritis nodosa associated with a low titre of MPO-ANCA]. *Ryumachi* 2000; **40**: 9-15 [PMID: 10783660]

13 **Iwamasa K**, Komori H, Niiya Y, Hasegawa H, Sakai I, Fujita S, Yoshida M, Nose M. [A case of polyarteritis nodosa limited to both calves with a low titer of MPO-ANCA]. *Ryumachi* 2001; **41**: 875-879 [PMID: 11729667]

14 **Tanaka M**, Matsuo K, Nakamura H, Ishikawa S, Matsuyama K. [Two cases of classical polyarteritis nodosa associated with MPO-ANCA]. *Nihon Jinzo Gakkai Shi* 2006; **48**: 371-376 [PMID: 16780107]

15 **Sakaguchi Y**, Uehata T, Kawabata H, Niihata K, Shimomura A, Suzuki A, Kaneko T, Shoji T, Shimazu K, Fushimi H, Tsu-

bakihara Y. An autopsy-proven case of myeloperoxidase-antineutrophil cytoplasmic antibody-positive polyarteritis nodosa with acute renal failure and alveolar hemorrhage. *Clin Exp Nephrol* 2011; **15**: 281-284 [PMID: 21161718 DOI: 10.1007/s10157-010-0386-9]

16 **Yamamoto T**, Matsuda J, Kadoya H, Mori D, Ito D, Namba T, Takeji M, Fukunaga M, Yamauchi A. A case of MPO-ANCA-positive polyarteritis nodosa complicated by exudative otitis media, mononeuritis multiplex, and acute renal failure. *Clin Exp Nephrol* 2011; **15**: 754-760 [PMID: 21611757 DOI: 10.1007/s10157-011-0457-6]

17 **Fujimoto S**, Watts RA, Kobayashi S, Suzuki K, Jayne DR, Scott DG, Hashimoto H, Nunoi H. Comparison of the epidemiology of anti-neutrophil cytoplasmic antibody-associated vasculitis between Japan and the U.K. *Rheumatology* (Oxford) 2011; **50**: 1916-1920 [PMID: 21798892 DOI: 10.1093/rheumatology/ker205]

18 **Kobayashi S**, Fujimoto S, Takahashi K, Suzuki K. Anti-neutrophil cytoplasmic antibody-associated vasculitis, large vessel vasculitis and Kawasaki disease in Japan. *Kidney Blood Press Res* 2010; **33**: 442-455 [PMID: 21071954 DOI: 10.1159/000320383]

19 **Lightfoot RW**, Michel BA, Bloch DA, Hunder GG, Zvaifler NJ, McShane DJ, Arend WP, Calabrese LH, Leavitt RY, Lie JT. The American College of Rheumatology 1990 criteria for the classification of polyarteritis nodosa. *Arthritis Rheum* 1990; **33**: 1088-1093 [PMID: 1975174]

20 **Guillevin L**, Cohen P, Mahr A, Arène JP, Mouthon L, Puéchal X, Pertuiset E, Gilson B, Hamidou M, Lanoux P, Bruet A, Ruivard M, Vanhille P, Cordier JF. Treatment of polyarteritis nodosa and microscopic polyangiitis with poor prognosis factors: a prospective trial comparing glucocorticoids and six or twelve cyclophosphamide pulses in sixty-five patients. *Arthritis Rheum* 2003; **49**: 93-100 [PMID: 12579599]

21 **Ebert EC**, Hagspiel KD, Nagar M, Schlesinger N. Gastrointestinal involvement in polyarteritis nodosa. *Clin Gastroenterol Hepatol* 2008; **6**: 960-966 [PMID: 18585977 DOI: 10.1016/j.cgh.2008.04.004]

P- Reviewers Camara CR, Grundmann RT
S- Editor Gou SX **L- Editor** O'Neill M **E- Editor** Lu YJ

Shirai et al. Journal of Neuroinflammation 2013, 10:128
http://www.jneuroinflammation.com/content/10/1/128

JNI JOURNAL OF NEUROINFLAMMATION

CASE REPORT Open Access

A novel autoantibody against ephrin type B receptor 2 in acute necrotizing encephalopathy

Tsuyoshi Shirai[1], Hiroshi Fujii[1*], Masao Ono[2], Ryu Watanabe[1], Yuko Shirota[1], Shinichiro Saito[1], Tomonori Ishii[1], Masato Nose[2] and Hideo Harigae[1]

Abstract

Acute necrotizing encephalopathy (ANE) is characterized by symmetrical brain necrosis, suggested to be due to breakdown of the blood–brain barrier (BBB). We experienced a rare case of ANE complicated with systemic lupus erythematosus (SLE), and found that the patient's serum (V10-5) had binding activity to human umbilical vein endothelial cells (HUVECs). By SARF (Serological identification system for Autoantigens using a Retroviral vector and Flow cytometry) method using V10-5 IgG, a clone bound to V10-5 IgG was isolated. This cell clone was integrated with cDNA identical to *EphB2*, which plays critical roles in neuronal cells and endothelial cells. HUVECs and human brain microvascular endothelial cells expressed EphB2 and the V10-5 IgG bound specifically to *EphB2*-transfected cells. Anti-EphB2 antibody was not detected in other SLE patients without ANE. In this report, we identified EphB2 as a novel autoantigen, and anti-EphB2 antibody may define a novel group of brain disorders. Anti-EphB2 antibody can interfere not only with endothelial cells including those of the BBB (acting as an anti-endothelial cell antibody), but also neuronal cells (acting as an anti-neuronal antibody) if the BBB has been breached. Future studies should determine the clinical prevalence and specificity of anti-EphB2 antibody, and the molecular mechanisms by which anti-EphB2 antibody mediates neuronal and vascular pathological lesions.

Keywords: Acute necrotizing encephalopathy, Autoantibody, Ephrin type B receptor 2, Serological identification system for Autoantigens using a Retroviral vector and Flow cytometry (SARF)

Background

A group of brain disorders involving autoantibodies targeting cell-surface or synaptic proteins has been identified. The antigens include N-methyl-D-aspartate receptor (NMDAR), α-amino-3-hydroxy-5-methyl-4-isoxazolepropionic acid receptor (AMPAR), γ-aminobutyric acid receptor-B (GABAB receptor), leucine-rich glioma-inactivated protein 1 (LGI1), contactin-associated protein-like 2 (Caspr2), glycine receptor (GlyR), and metabotropic glutamate receptor mGluR5 [1].

Autoantibodies cause tissue damage through a number of mechanisms. Especially, cell-surface target antigens are susceptible to disruption by autoantibodies, and syndromes mediated by these autoantibodies often mimic animal models with genetic or pharmacological disruption of these molecules [1]. Identifying these autoantigens would be helpful in understanding the pathophysiology of these syndromes.

Acute necrotizing encephalopathy (ANE) is a rare type of acute encephalopathy first described in Japan. The diagnosis is based on the topographic distribution and evolution of symmetric lesions visualized by computed tomography (CT) and magnetic resonance imaging (MRI) in the bilateral thalami and other specific brain areas [2]. Although the pathogenesis remained obscure, vasculopathy with breakdown of the blood–brain barrier (BBB) was suggested [3].

Recently, we established a novel method to identify cell-surface autoantigens, which we named Serological identification system for Autoantigens using a Retroviral vector and Flow cytometry (SARF) [4,5]. Using SARF, we successfully identified ephrin type B receptor 2 (EphB2), which has critical functions in neuronal and endothelial cells (ECs) [6], as a target of autoantibody from a patient with ANE complicated with systemic lupus erythematosus (SLE).

* Correspondence: hfujii@med.tohoku.ac.jp
[1]Department of Hematology and Rheumatology, Tohoku University Graduate School of Medicine, 1-1 Seiryo-cho, Aoba-ku, Sendai, Miyagi 980-8574, Japan
Full list of author information is available at the end of the article

Methods

Source of human serum

Forty-eight patients with SLE (44 female and 4 male patients) diagnosed according to the 1997 revised criteria for the classification [7] were enrolled in this study. The patients gave written consent after the purpose and potential risks involved in the study were explained. The study protocol complied with the principles of the Declaration of Helsinki and was approved by the Ethics Committee of Tohoku University Graduate School of Medicine.

Cell culture

Human umbilical vein ECs (HUVECs), Plat-E packaging cells, rat myeloma cells: YB2/0, and medium were purchased and grown as described previously [4]. Human brain microvascular ECs (HBMECs) and medium were purchased from Cell Systems (Kirkland, WA, USA).

Flow cytometry

Binding activities of antibodies to the surface of ECs and EphB2 were measured and analyzed as described previously [4]. Briefly, aliquots of 1×10^5 cells/tube were incubated in blocking buffer with primary antibodies at 4°C for 30 minutes. After washing, cells were incubated with secondary antibodies and 7-amino-actinomycin D (7-AAD) (BD Biosciences, Bedford, MA, USA) at 4°C for 30 minutes and analyzed by flow cytometry.

Goat anti-human EphB2 antibody was purchased from R&D Systems (Minneapolis, MN, USA), and recombinant EphB2 was purchased from Sino Biological (Beijing, China).

SARF

Generation of HUVEC cDNA library and screening of cDNA were performed as described previously [4]. Briefly, the HUVEC cDNA library was retrovirally transfected into the YB2/0 cells. YB2/0 cells expressing the HUVEC cDNA library were incubated with serum IgG and fluorescein isothiocyanate (FITC)-labeled secondary antibody. Cells showing a high level of FITC fluorescence were sorted with FACSAriaII (Becton Dickinson, Franklin Lakes, NJ, USA). Sorted cells were kept in culture until the cell number increased sufficiently for the next round of sorting. Subcloning of cells was performed by the limiting dilution method. Total RNAs of cloned cells and unsorted cells were generated and subjected to microarray analysis (GeneChip Human Genome U133 Plus 2.0 Array; Affymetrix, Santa Clara, CA, USA).

Expression of EphB2 in YB2/0 cells

The full-length EphB2 fragment was amplified by PCR from genomic DNA of EphB2-expressing YB2/0 clone sorted as described above, using Phusion High-Fidelity DNA Polymerase (Finnzymes, Keilaranta, Espoo, Finland). Primer sequences were as follows: 5′-AAGCGCAGC CATGGCTCT-3′, 3′-AGGCAGGTGAATGTCAAACC-5′. EphB2 fragment was inserted into the pMX-IRES-GFP vector (Cell Biolabs, San Diego, CA, USA).

Case presentation

Case of ANE complicated with SLE

A 39-year-old Japanese woman was admitted to our hospital because of coma. One day previously, she had been admitted to another hospital because of diarrhea lasting three days. The next morning, she suddenly fell into a coma and developed quadriplegia, and was transferred to our hospital. On admission, her consciousness was GCSE1V1M2, both pupil sizes were 3 mm, and both pupillary light reflexes were absent. Decorticate rigidity and Babinski reflex were present. The cerebrospinal fluid (CSF) showed normal glucose and no pleocytosis, but the total protein level was elevated to 316 mg/dL. Laboratory tests indicated lymphopenia (410/μL), and elevated levels of aspartate aminotransferase (AST; 136 IU/L), lactate dehydrogenase (LDH; 740 IU/L), and C-reactive protein (CRP; 0.9 mg/dL). Serum complement levels were decreased as follows: C3, 42 mg/dL; C4, 5.3 mg/dL CH50, 10.8 U/mL. Antinuclear antibody (ANA) (×640, speckled) and anti-Sm antibody (48.7 index) were positive, but anti-dsDNA antibody and anti-phospholipid antibodies were negative. Tests for infections and urine were negative. CT showed low density area in the bilateral thalami, basal ganglia, medial temporal lobe, and brainstem (Figure 1A). MRI revealed high signal intensity in T2 (Figure 1B) and diffusion-weighted images in the same areas as described above (Figure 1C). A diagnosis of neuropsychiatric SLE (NPSLE) manifesting ANE was made based on the clinical, serological, and imaging findings. Despite extensive treatment, her consciousness did not recover, and she remained in a permanently vegetative state.

Identification of EphB2 as a novel cell-surface autoantigen

Serum from this patient (V10-5) showed strong binding activity to HUVECs (anti-endothelial cell antibody (AECA) activity) (Figure 2A). Using SARF, the YB2/0 cell line expressing HUVEC cDNA was incubated with V10-5 IgG and FITC-conjugated secondary antibody, and cells with strong FITC signals were sorted by flow cytometry (Figure 2B). After cell expansion, we repeated three more rounds of cell sorting. After the fourth round of sorting, cells bound to V10-5 IgG were markedly increased (Figure 2C, upper). Then, one clone (C17) was established from the V10-5 IgG-binding cell population by the limiting dilution method (Figure 2C. lower).

Microarray analysis of unsorted YB-2/0 and C17 indicated that the signal of EphB2 was significantly increased

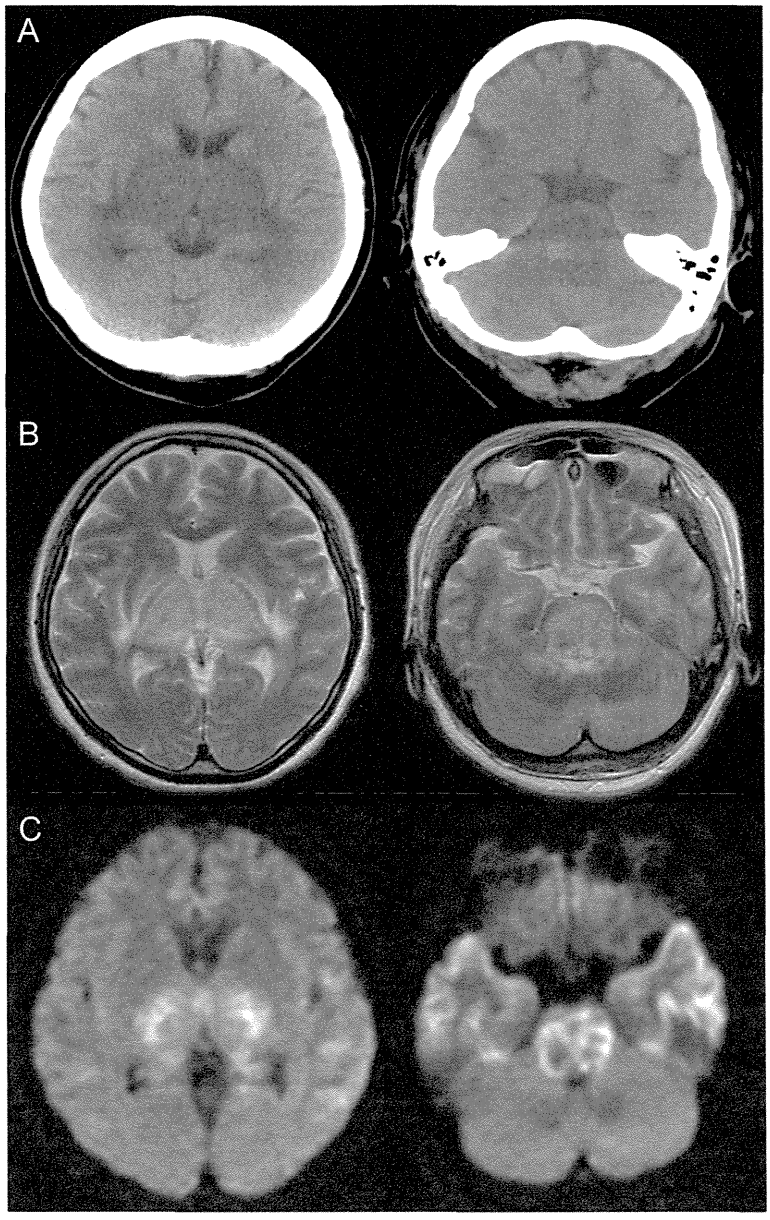

Figure 1 Clinical imaging. (A) CT showed low density area in the bilateral thalami, basal ganglia, medial temporal lobe, and brainstem. The brainstem was swollen, and high density area was observed in the pons. **(B)** MRI (T2-weighted image) revealed high signal intensity in the bilateral thalami, basal ganglia, medial temporal lobe, and brainstem. **(C)** MRI (diffusion-weighted image) also showed high signal intensity in the same area.

($2^{6.16}$-fold) in C17 compared to unsorted cells, and we confirmed that the *EphB2* cDNA was inserted into the genomic DNA of the V10-5-C17 clone by PCR (Figure 2D). We also confirmed the expression of EphB2 on the V10-5-C17 clone by flow cytometry (Figure 2E). Next, we generated an expression vector for EphB2, which was transfected into YB2/0 cells. V10-5 IgG showed significant binding activity to EphB2-expressing YB2/0 cells (Figure 2F), indicating that V10-5 IgG has anti-EphB2 activity. Thus, EphB2 was identified as a novel autoantigen in a patient with ANE complicated with SLE.

Flow cytometry indicated that HUVECs and HBMECs also expressed EphB2 on their cell surfaces (Figure 3A). We conducted inhibition tests to determine whether the AECA activity of V10-5 IgG was due to anti-EphB2 activity. Anti-HBMEC activity of V10-5 IgG was inhibited by addition of recombinant EphB2 (Figure 3B). We also analyzed the IgG subclasses of anti-EphB2 antibody by flow

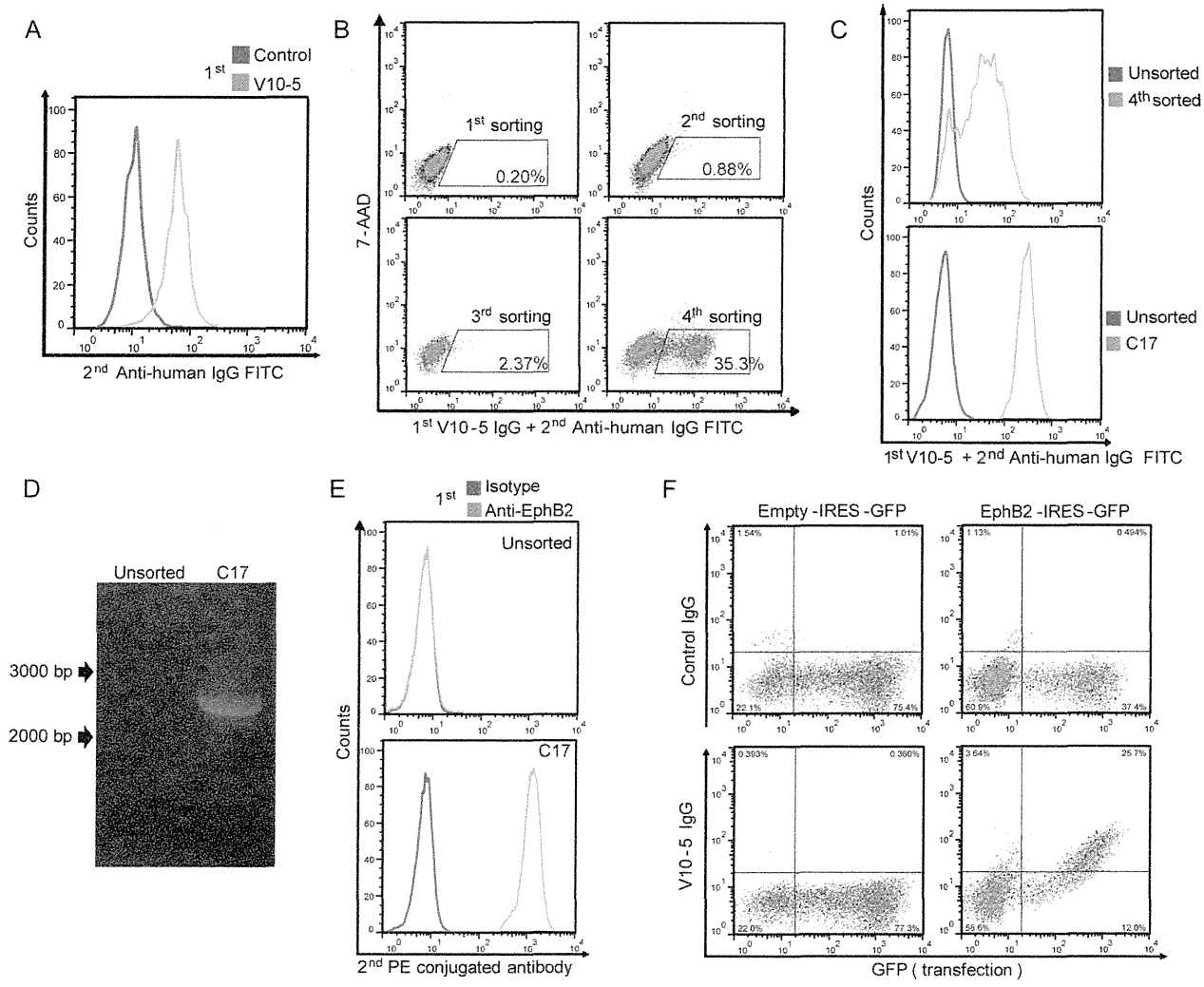

Figure 2 Identification of ephrin type B receptor 2 (EphB2) as a novel autoantigen. (A) Nonpermeabilized human umbilical vein endothelial cells (HUVECs) were stained with 0.5 mg/mL of IgG of control or V10-5 followed by secondary antibody and analyzed by flow cytometry. **(B)** HUVEC cDNA-expressing cells were stained with 0.5 mg/mL of V10-5 IgG followed by secondary antibody, and cells in the positive fraction were sorted (squares). **(C)** Unsorted cells and those at the fourth round of sorting (upper), and unsorted and cloned cells from those at the fourth round of sorting, C17 (lower), were stained with 0.5 mg/mL of V10-5 IgG followed by secondary antibody, and analyzed by flow cytometry. **(D)** *EphB2* cDNA fragments inserted into the genomic DNA of C17 were amplified, and PCR products were electrophoresed on a 0.8 % agarose gel. **(E)** Unsorted and C17 were stained with isotype control or anti-EphB2 antibody, followed by secondary antibody and analyzed by flow cytometry. **(F)** Expression vector, empty-IRES-GFP, or EphB2-IRES-GFP was transfected into YB 2/0 cells, and the cells were stained with 0.5 mg/mL of control IgG or V10-5 IgG, followed by secondary antibody and analyzed by flow cytometry.

cytometry. IgGs with anti-EphB2 activity were IgG1, IgG2, and IgG3 (Figure 3C).

Although we measured anti-EphB2 activity among 47 SLE patients (nine patients had been diagnosed with NPSLE, none of them presented ANE) who had AECA activities, anti-EphB2 antibody was not detected in any other SLE patients examined.

Discussion

Identification of EphB2 as a novel autoantigen may be important in clarifying the pathogenesis of ANE because anti-EphB2 antibody has potential to play pathogenic roles in neuronal and vascular lesions.

ANE has a high mortality rate and is usually preceded by infections, such as influenza, with the signs of brain dysfunction appearing a few days later [8]. It is characterized by symmetrical brain necrosis, which involves the thalamus followed by the tegmentum of the pons and other regions, and these are demonstrated by CT and MRI [3]. Neuropathologically, the lesions tend to spread along small blood vessels, and the extent of the lesions appears to be determined by the spread of edema fluid. These observations indicate the vasogenic nature

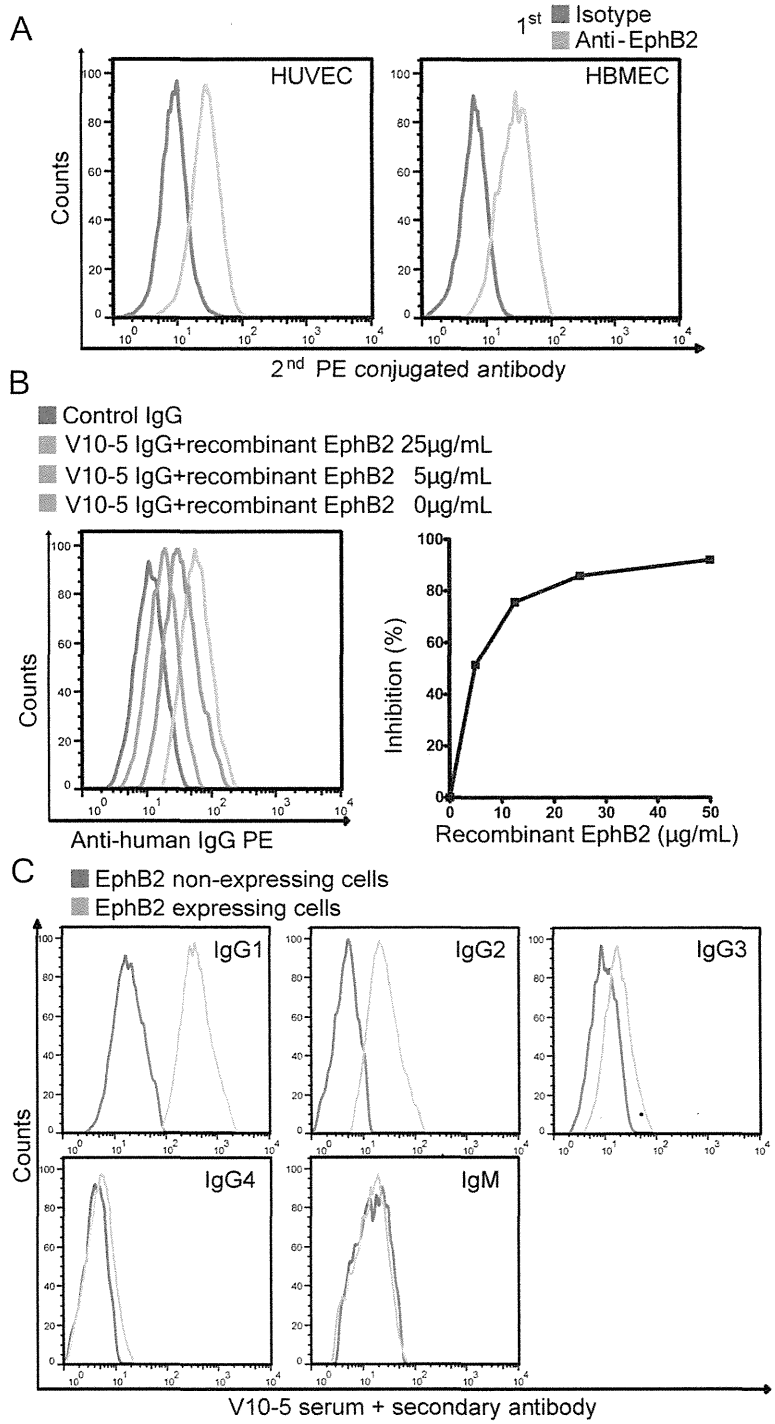

Figure 3 Confirmation of anti-EphB2 activity of V10-5 IgG. (A) Nonpermeabilized human umbilical vein endothelial cells (HUVECs) and human brain microvascular cells (HBMECs) were stained with isotype control or anti-EphB2 antibody followed by secondary antibody, and analyzed by flow cytometry. **(B)** Inhibition tests of binding activities to HBMECs were performed using V10-5 IgG with soluble EphB2 at the indicated concentrations. Control indicates binding activity of IgG from healthy donor to HBMECs. **(C)** EphB2-expressing or non-expressing YB2/0 cells were stained with 1:10 diluted V10-5 serum followed by secondary antibody against human IgG1, IgG2, IgG3, IgG4, or IgM, and analyzed by flow cytometry.

of edema-necrosis in ANE, resulting from local breakdown of the BBB [8]. EC necrosis and inflammatory fibrinoid vasculitis have also been reported [9].

Although our patient showed characteristic features of ANE, this is a very rare complication of SLE; to our knowledge, no other cases of SLE manifesting ANE have been reported to date. Although some previous reports indicated the absence of ANA in ANE [2], the correlation between SLE and ANE is uncertain.

Eph receptors belong to one of the largest families of tyrosine kinases. They are known to have diverse functions in neural development, cell morphogenesis, tissue patterning, angiogenesis, and neural plasticity [6]. Among them, the critical roles of EphB2 in the nervous system have recently been clarified. The important functions of EphB2 include regulation of NMDAR-dependent Ca^{2+} influx and downstream transcription factors in neuronal cells [10], and the involvement in neurological diseases, including Alzheimer's disease, anxiety, and anti-NMDA encephalitis has been reported [11-13]. We performed an immunohistochemical study of mouse brain tissues using a commercially available anti-EphB2 antibody. As a result, we identified positive reactions on neural cells and glia in the cerebral cortex and also ECs in the subarachnoid regions (data not shown). Further studies would be done to investigate whether the reactivity of the patient's antibodies with brain is abrogated by immunoadsorption with EphB2 or in EphB2 knockout mice tissues. Interestingly, EphB2 is also expressed on ECs and is required for EC formation of cord-like structures [14].

Thus, anti-EphB2 antibody could potentially interfere not only with ECs including those of the BBB (acting as an AECA), but also neuronal cells (acting as an anti-neuronal antibody) if the BBB has been breached. Taken together, the possible suspected pathomechanisms are 1) anti-EphB2 antibody damages vascular ECs, which results in breakdown and increased permeability of BBB; 2) anti-EphB2 antibody exudated into brain tissue binds neurons and glia, which causes neuronal dysfunction and brain necrosis.

In the present study, anti-EphB2 antibody was not detected in any other patients with SLE, none of whom manifested ANE. Although we did not evaluate the prevalence of anti-EphB2 antibody in other ANE patients because of its rarity, anti-EphB2 antibody may define a novel group of brain disorders the clinical manifestations of which are similar to those of ANE. If this is the case, anti-EphB2 antibody may be a useful biomarker, and provide new insight into such brain disorders.

Conclusion

We identified EphB2 as a novel autoantigen in a patient with ANE complicated with SLE. Anti-EphB2 antibody may have dual activity as an AECA and an anti-neuronal antibody. Further studies are needed to determine the clinical prevalence and specificity of anti-EphB2 antibody, and the molecular mechanisms by which anti-EphB2 antibody mediates neuronal and vascular pathological lesions.

Consent

Written informed consent was obtained from the next of kin of this patient for publication of this case report and any accompanying images because consciousness of this patient did not recover. A copy of the written consent is available for review by the Editor-in-Chief of this journal.

Abbreviations

AECA: Anti-endothelial cell antibody; AMPAR: α-amino-3-hydroxy-5-methyl-4-isoxazolepropionic acid receptor; ANA: Antinuclear antibody; ANE: Acute necrotizing encephalopathy; AST: Aspartate aminotransferase; BBB: Blood–brain barrier; Caspr2: Contactin-associated protein-like 2; CRP: C-reactive protein; CSF: Cerebrospinal fluid; CT: computed tomography; ECs: Endothelial cells; EphB2: Ephrin type B receptor 2; FITC: Fluorescein isothiocyanate; GABAB: γ-aminobutyric acid receptor-B; GlyR: Glycine receptor; HBMECs: Human brain microvascular endothelial cells; HUVECs: Human umbilical vein endothelial cells; LDH: Lactate dehydrogenase; LGI1: Leucine-rich glioma-inactivated protein 1; mGluR: Metabotropic glutamate receptor; MRI: Magnetic resonance imaging; NMDAR: N-methyl-D-aspartate receptor; NPSLE: Neuropsychiatric systemic lupus erythematosus; PCR: Polymerase chain reaction; SARF: Serological identification system for Autoantigens using a Retroviral vector and Flow cytometry; SLE: Systemic lupus erythematosus; 7-AAD: 7-amino-actinomycin D.

Competing interests

The authors declare that they have no competing interests.

Authors' contributions

TS carried out the molecular biological studies, flow cytometry, clinical evaluation, and drafted the manuscript. HF, MO, and MN participated in design of the study, performed the molecular biological studies, and helped to draft the manuscript. RW, YS, SS, and TI participated in the design of the study and helped to draft the manuscript. HH conceived the study, participated in its design and coordination, and helped to draft the manuscript. All authors have read and approved the final manuscript.

Acknowledgements

We thank the staff of the Department of Hematology and Rheumatology, and the Department of Neurology, Tohoku University, for help and discussion.

Author details

[1]Department of Hematology and Rheumatology, Tohoku University Graduate School of Medicine, 1-1 Seiryo-cho, Aoba-ku, Sendai, Miyagi 980-8574, Japan. [2]Department of Histopathology, Tohoku University Graduate School of Medicine, 1-1 Seiryo-cho, Aoba-ku, Sendai, Miyagi 980-8574, Japan.

Received: 29 June 2013 Accepted: 1 October 2013
Published: 18 October 2013

References

1. Lancaster E, Dalmau J: **Neuronal autoantigens - pathogenesis, associated disorders and antibody testing.** *Nat Rev Neurol* 2012, **8**:380–390.
2. Mastroyianni SD, Gionnis D, Voudris K, Skardoutsou A, Mizuguchi M: **Acute necrotizing encephalopathy of childhood in non-Asian patients: report of three cases and literature review.** *J Child Neurol* 2006, **21**:872–879.
3. Spalice A, Del Balzo F, Nicita F, Papetti L, Ursitti F, Salvatori G, Zicari AM, Properzi E, Duse M: **Teaching NeuroImages: acute necrotizing encephalopathy during novel influenza A (H1N1) virus infection.** *Neurology* 2011, **77**:e121.